Structural Biology

DOI: 10.1002/ange.201409679

W246$^{6.48}$ Opens a Gate for a Continuous Intrinsic Water Pathway during Activation of the Adenosine A_{2A} Receptor**

Shuguang Yuan, Zhenquan Hu, Slawomir Filipek, and Horst Vogel**

Abstract: *The question how G-protein-coupled receptors transduce an extracellular signal by a sequence of transmembrane conformational transitions into an intracellular response remains to be solved at molecular detail. Herein, we use molecular dynamics simulations to reveal distinct conformational transitions of the adenosine A_{2A} receptor, and we found that the conserved W246$^{6.48}$ residue in transmembrane helix TM6 performs a key rotamer toggle switch. Agonist binding induces the sidechain of W246$^{6.48}$ to fluctuate between two distinct conformations enabling the diffusion of water molecules from the bulk into the center of the receptor. After passing the W246$^{6.48}$ gate, the internal water molecules induce another conserved residue, Y288$^{7.53}$, to switch to a distinct rotamer conformation establishing a continuous transmembrane water pathway. Further, structural changes of TM6 and TM7 induce local structural changes of the adjacent lipid bilayer.*

G-protein-coupled receptors (GPCRs) mediate most of our physiological responses to external stimuli including neurotransmitters, hormones, and diverse environmental signals.[1] As GPCRs are involved in many diseases and neurological disorders, they are targets for many presently used medicines and are of utmost interest for the development of novel therapeutic compounds.[1c,2] Despite of recent progress in determining high-resolution structures of GPCRs, the central question remains to be clarified how ligand binding to a receptor induces a sequence of conformational changes in the protein mediating transmission of the signal across the membrane and finally leading to binding and activation of a G protein at the intracellular side of the receptor approximately 3 nm away from the ligand binding site. Molecular modeling and molecular dynamics (MD) simulations can elucidate important steps of GPCR activation, which are not accessible by experiments.[3,4] For example, to resolve the important role that protein intrinsic water molecules play in GPCR mediated transmembrane signaling.[3,5,6]

Herein we concentrate on the role of intrinsic water molecules for signal transmission by the adenosine A_{2A} receptor ($A_{2A}R$), a prototypical member of the rhodopsin-like class A GPCR family.[7] The $A_{2A}R$ is expressed in a wide variety of tissues and is of functional importance in many central metabolic processes, such as regulation of myocardiac function and in metabolic disorders.[7,8] The recently released 1.8 Å resolution crystal structure of $A_{2A}R$ revealed a network of water molecules inside the receptor.[6] This raises a question, how the intrinsic water molecules are coupling to and affecting the GPCR activation process, which presently cannot be answered from static X-ray structure analyses. To solve this problem, we first employed all-atom, 6.4 μs MD simulations of complexes of $A_{2A}R$ with bound antagonist ZMA ($A_{2A}R$/ZMA) and agonist NECA[9] ($A_{2A}R$/NECA; Scheme 1). In the next step we simulated the activated receptor as a complex with a peptide fragment of the corresponding G_α protein at the cytoplasmic side. All the simulations started from the 1.8 Å high-resolution crystal structure of the $A_{2A}R$[6] (protein data bank code (pdb): 4EIY) including 57 internal water molecules and a sodium ion at the receptor's allosteric site. Previously, we found that the structures of GPCRs in their inactive states comprise internally two distinct layers, HL1 and HL2, of hydrophobic amino acid residues which exclude water molecules in these regions; binding of an agonist to the receptor induces internal protein structural changes allowing the entrance of water into

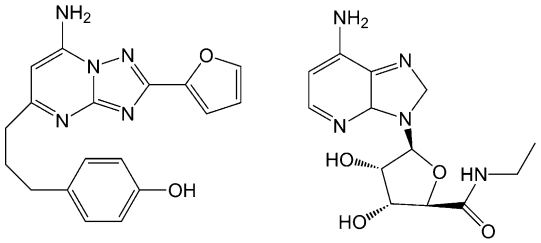

ZMA (antagonist) NECA (agonist)

Scheme 1. $A_{2A}R$ ligands used in MD simulations.

[*] Dr. S. Yuan, Prof. H. Vogel
Laboratory of Physical Chemistry of Polymers and Membranes
Ecole Polytechnique Fédérale de Lausanne (EPFL)
Lausanne (Switzerland)
E-mail: shuguang.yuan@gmail.com
horst.vogel@epfl.ch
Dr. Z. Hu
Department of Pharmaceutical Sciences
University of Basel (Switzerland)
Prof. S. Filipek
Laboratory of Biomodeling, Faculty of Chemistry & Biological and Chemical Research Centre, University of Warsaw
Warsaw (Poland)

[**] We thank the Shanghai Supercomputer Center for supporting the major computing part of this project; part of the work was done at Interdisciplinary Centre for Mathematical and Computational Modeling in Warsaw (grant G07-13). S.F. received funding from National Center of Science, Poland, grant no. 2011/03/B/NZ1/03204. Research in H.V.'s group was supported by the Swiss National Science Foundation (grant 31003A-133141), by the European Community (project SynSignal, grant FP7-KBBE-2013-613879), and internal funds of the EPFL. H.V. and S.F. participate in the European COST Action CM1207 (GLISTEN).

Supporting information for this article is available on the WWW under http://dx.doi.org/10.1002/anie.201409679.

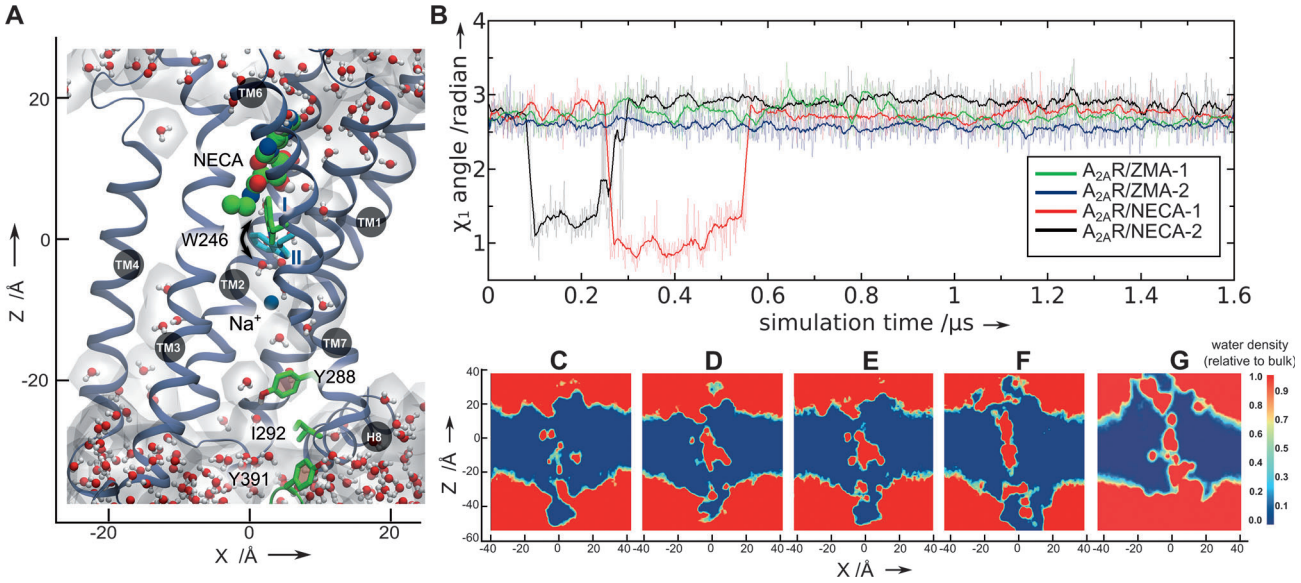

Figure 1. Conformational fluctuations of W246$^{6.48}$ and distribution of water molecules in the complex A_{2A}R/NECA. A) 3D structure of A_{2A}R with bound NECA. W246$^{6.48}$ fluctuates between two distinct conformations (I and II) during the activation process of A_{2A}R. At the end of the 1.6 μs MD simulations, the activated receptor in the A_{2A}R/NECA complex shows a continuous pathway of water molecules (red dots) mediated by a sodium ion at the allosteric site. B) Rotamer χ_1 angle of W246$^{6.48}$ in two independent MD simulations. In the antagonist-bound complex A_{2A}R/ZMA (green and blue, two independent MD simulations), the χ_1 angle of W246$^{6.48}$ remains stable during the two 1.6 μs long MD simulations. In the agonist-bound complex A_{2A}R/NECA (red and black, two independent MD simulations), the χ_1 angle of W246$^{6.48}$ fluctuates in each particular simulation between two distinct states at the time scale 0.1–0.6 μs ($\chi_1 = 2.75 \pm 0.25$, conformation I; $\chi_1 = 1 \pm 0.2$, conformation II). C)–G) Average water density at time C) 0.1–0.2 μs, D) 0.2–0.3 μs, E) 0.3–0.4 μs, F) 0.4–0.5 μs, G) 1.5–1.6 μs. Red = high water density, blue = low water density.

the hydrophobic regions and the formation of a continuous transmembrane water pathway within the receptor.[3b]

Herein, we show that W246$^{6.48}$ (Ballesteros/Weinstein numbering[10]) in TM6, which usually interacts with the agonist molecules at the orthosteric site directly, is a "key" residue for the rotamer toggle switches.[4f] As depicted in Figure 1 A,B, in the agonist bound complex A_{2A}R/NECA, the sidechain of W246$^{6.48}$ fluctuates between two distinct rotamer conformations during the initial 0.1–0.6 μs period of our MD simulations. For clarity, we first focus on the simulations of A_{2A}R/NECA in Figure 1 B.

Interestingly, the water density inside the receptor increases gradually as the conformational switching of W246$^{6.48}$ took place (Figure 1 C–F). Both hydrophobic layers, HL1 and HL2, shrink steadily over this time, and finally a continuous water pathway is established (Figure 1 A and G). Interestingly, W246$^{6.48}$ remained for about 0.2–0.3 μs in the rotamer conformation II and then switched back to its original inactive conformation I, which is in agreement with observations made elsewhere for fully activated GPCRs.[11] Such a phenomenon was also found in all-atom long-time simulations of other GPCRs.[3a,12]

Besides the rotamer switches, bending of helices TM6 and TM7 are further hallmarks of GPCR activation.[4f,13] They are also observed in MD simulations.[4a,f,12a] As shown in Figure 2 A, at the end of MD simulations in the antagonist complex A_{2A}R/ZMA, the helix kink of TM7 is almost identical to that in the initial crystal structure. However, when agonist was bound to the receptor, a helix movement took place at residues 276–283 in TM7 (Figure 2 B,C). This helix segment moved about 3 Å towards the center of the transmembrane receptor part. Similar movements also occurred in TM6 (Figure S1 in the Supporting Information). In the complex A_{2A}R/NECA, the bending of TM6 was clearly observed in the region of residues 222–232, which is close to the G-protein binding site at the cytoplasmic side. However, such changes were not present in antagonist bound A_{2A}R/ZMA complex. Taken together, these observations are in close agreement with crystal structures of activated GPCRs.[1a,4f,9,14]

The analysis of the interaction between residue side chains (Figure 2 D,E) shows that in the antagonist bound complex A_{2A}R/ZMA most of the residues inside the receptor contacting multiple neighbors as depicted in a big circle in Figure 2 D. The MD simulations revealed also residues without any internal protein contacts, most of which are located on the receptor surface or in loops (Figure 2 D bottom, scattered dots). By contrast, in the agonist bound complex A_{2A}R/NECA (Figure 2 E), the interactions between side chains inside the receptor were disrupted by helix bents, accompanied by water influx, which forced side chain interactions to occur in small local groups requiring larger space. As before, residues without any contact were preferentially found on the surface of the receptor or in loops.

Interestingly, the distinct conformational changes in A_{2A}R induced by various ligands lead to distinct local patterns of bilayer deformations around the receptor. Such differences are results of hydrophobic lipid tails tending to match the hydrophobic surfaces at the different TM helixes. For example, the hydrophobic lipid bilayer surrounding the inactive A_{2A}R/ZMA complex (Figure 2 F) is thicker than that of the activated A_{2A}R/NECA complex (Figure 2 G),

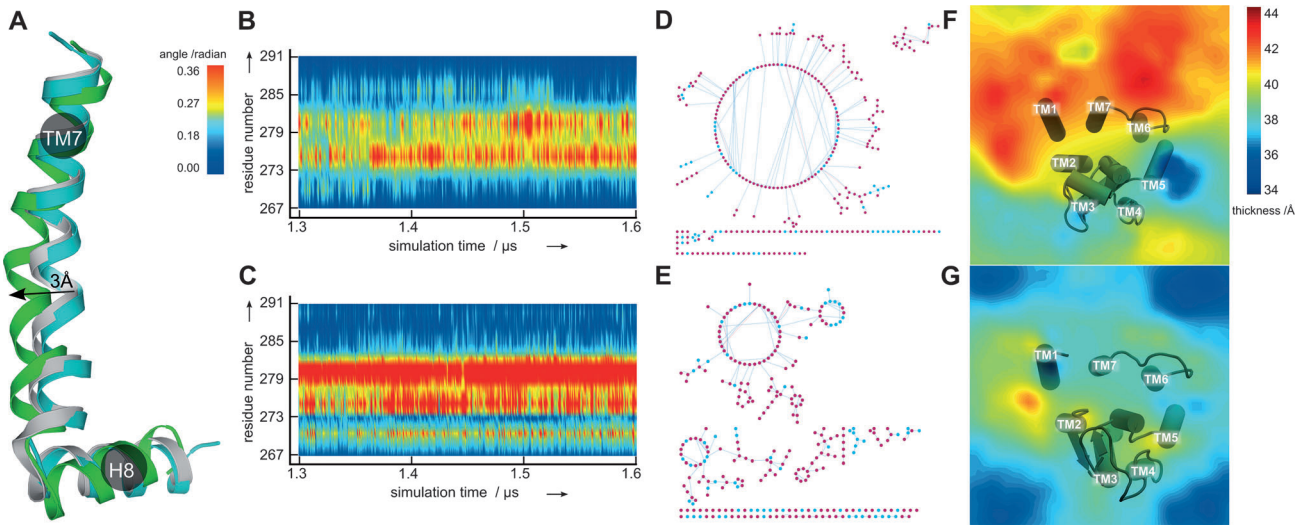

Figure 2. Helix bending of TM7 induces activation of $A_{2A}R$. A) Superimposed TM7 helices arising from the resting-state crystal structure (gray) and the structures at the end of 6.4 µs MD simulations of $A_{2A}R$/NECA (green), and $A_{2A}R$/ZMA (cyan). The transition from an inactive receptor (bound antagonist) to an activated receptor (bound agonist) is accompanied by 3 Å movement of the central, bent region of TM7 indicated by the arrow. B) Bending of TM7 in $A_{2A}R$/ZMA. C) Bending of TM7 in $A_{2A}R$/NECA. In B,C, the bending is characterized as the local angle of the indicated three successive amino acid residues given in a color scale (left of (B)). D) Side-chain interactions in $A_{2A}R$/ZMA during final 0.1 µs MD simulations. Residues in the helix and in the loop are red and cyan dots, respectively. Line connections indicate residues' contact (for details, see Supporting Information). E) Side-chain interactions in $A_{2A}R$/NECA during final 0.1 µs MD simulations (for details, see Supporting Information). F) Average hydrophobic thickness profile of the lipid bilayer surrounding $A_{2A}R$/ZMA during final 0.1 µs MD simulations. G) Average hydrophobic thickness profile of the lipid bilayer surrounding $A_{2A}R$/NECA during final 0.1 µs MD simulations.

especially in the region next to TM6 and TM7. These observations are in agreement with our findings that TM6 and TM7 show much more pronounced bents in the activated ($A_{2A}R$/NECA) than in the inactive ($A_{2A}R$/ZMA) receptor state which were matched by the hydrophobic lipid tails leading to a local reduction of the lipid bilayer thickness. The local changes of the bilayer structure might in turn have a profound influence on the receptor properties, for example inducing receptor dimerization or oligomerization.[15] Such mutual influence between membrane proteins and their surrounding lipids is widely discussed to be a central mechanism for the regulation of membrane structure and function.[16]

In conclusion, our all-atom long-time scale MD simulations revealed a central signal transmission switch during the initial stages of activation of the $A_{2A}R$ (Figure 3). Our results show that the activation process of $A_{2A}R$ proceeds in the following steps: First, the binding of an agonist molecule NECA at the orthosteric site of the receptor leads to a structural rotation transition in the side chain of $W246^{6.48}$. This movement opens a gate allowing the diffusion of water molecules from the bulk phase towards the central, internal space of the receptor, with the mediating help of a sodium ion at the allosteric receptor site.[3a,5a] During this motion of water molecules the other highly conserved residue, $Y288^{7.53}$ at the NPxxY motif[3b] close to the G-protein binding site, also performs a structural rotation transition during GPCR activation (Figure S2A). Now, in the present context, it leads to a coherent mechanism in which the incoming water molecules after passing the $W246^{6.48}$ gate induce $Y288^{7.53}$ to switch to a distinct rotamer conformation, which finally establishes a continuous transmembrane pathway of water

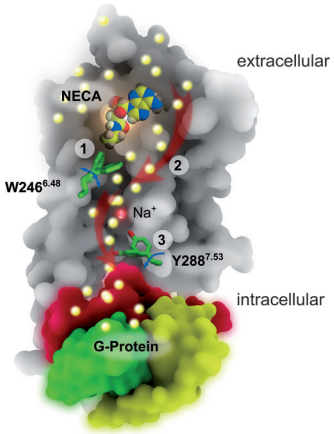

Figure 3. Formation of a continuous water channel during transmembrane signaling in the $A_{2A}R$ proceeds in a sequence of steps: 1) Binding of the agonist NECA at the orthosteric site induces $W246^{6.48}$ rotational fluctuations. 2) Water molecules from the bulk phase flow into the receptor (upper red arrow). 3) The movement of water molecules is mediated by a sodium ion to induce conformational switching of $Y288^{7.53}$ and in turn the formation of a continuous water pathway across the receptor (lower red arrow). Further movement of water molecules leads to bending of TM6 and TM7 enabling G-protein binding and activation at the cytoplasmic side of the receptor.

molecules. In addition, the successive movement of water molecules induces the structural changes of TM6 and TM7, first bending and then rotation, which finally enable binding and activation of G-proteins at the intracellular site of $A_{2A}R$. During this process, the conformational changes of the receptor couple to the lipid membrane and force the thickness of the hydrophobic part of the lipids close to TM6 and TM7 to

shrink noticeably which in turn could have substantial consequences on the receptor's function.

Experimental Section

The membrane system was built by g membed[17] tool in Gromacs[18] V4.6.3 with receptor crystal structure pre-aligned in the OPM (orientations of proteins in membranes) database.[19] Pre-equilibrated 132 POPC lipids coupled with 9200 TIP3P water molecules in a periodic box of $70 \times 70 \times 98$ Å were used to build the protein/membrane system. The protein was modeled using Amber99SB-ILD force field[20] with improved side-chain torsion potentials of Amber99SB force field; the POPC lipids were modeled using the Amber Slipids force field[21] parameter set; the ligands were modeled using the Amber GAFF small-molecule force field.[22] Next, an additional 40 ns constrained equilibration was performed at constant pressure and temperature (NPT ensemble; 310 K, 1 bar), and the force constant was gradually changed from 10 kcal mol^{-1} to 0 kcal mol^{-1}. The results obtained from MD simulations were analyzed in Gromacs[18] and VMD.[23] The water density was calculated in Gridcount,[24] a patched tool in Gromacs, and the calculations were performed based on MD simulation trajectories from each case. The bending of helix was calculated in Bendix[25] with default settings.

Received: October 1, 2014
Published online: November 17, 2014

Keywords: G-protein-coupled receptor · molecular dynamics simulations · molecular switches · signal transduction · water channel

[1] a) A. J. Venkatakrishnan, X. Deupi, G. Lebon, C. G. Tate, G. F. Schertler, M. M. Babu, *Nature* **2013**, *494*, 185–194; b) M. P. Bokoch, Y. Z. Zou, S. G. F. Rasmussen, C. W. Liu, R. Nygaard, D. M. Rosenbaum, J. J. Fung, H. J. Choi, F. S. Thian, T. S. Kobilka, J. D. Puglisi, W. I. Weis, L. Pardo, R. S. Prosser, L. Mueller, B. K. Kobilka, *Nature* **2010**, *463*, 108–121; c) D. M. Rosenbaum, S. G. Rasmussen, B. K. Kobilka, *Nature* **2009**, *459*, 356–363; d) K. P. Hofmann, P. Scheerer, P. W. Hildebrand, H. W. Choe, J. H. Park, M. Heck, O. P. Ernst, *Trends Biochem. Sci.* **2009**, *34*, 540–552; e) B. G. Tehan, A. Bortolato, F. E. Blaney, M. P. Weir, J. S. Mason, *Pharmacol. Ther.* **2014**, *143*, 51–60; f) K. Palczewski, T. Orban, *Annu. Rev. Neurosci.* **2013**, *36*, 139–164.

[2] a) B. C. Heng, D. Aubel, M. Fussenegger, *Biotechnol. Adv.* **2013**, *31*, 1676–1694; b) J. S. Mason, A. Bortolato, M. Congreve, F. H. Marshall, *Trends Pharmacol. Sci.* **2012**, *33*, 249–260.

[3] a) S. Yuan, H. Vogel, S. Filipek, *Angew. Chem. Int. Ed.* **2013**, *52*, 10112–10115; *Angew. Chem.* **2013**, *125*, 10299–10302; b) S. Yuan, S. Filipek, K. Palczewski, H. Vogel, *Nat. Commun.* **2014**, *5*, 4733.

[4] a) R. O. Dror, D. H. Arlow, D. W. Borhani, M. O. Jensen, S. Piana, D. E. Shaw, *Proc. Natl. Acad. Sci. USA* **2009**, *106*, 4689–4694; b) R. O. Dror, D. H. Arlow, P. Maragakis, T. J. Mildorf, A. C. Pan, H. Xu, D. W. Borhani, D. E. Shaw, *Proc. Natl. Acad. Sci. USA* **2011**, *108*, 18684–18689; c) S. Yuan, U. Ghoshdastider, D. Latek, B. Trzaskowski, A. Debinski, S. Filipek, *PloS one* **2012**, e47114; d) Z. Yang, K. Lasker, D. Schneidman-Duhovny, B. Webb, C. C. Huang, E. F. Pettersen, T. D. Goddard, E. C. Meng, A. Sali, T. E. Ferrin, *J. Struct. Biol.* **2012**, *179*, 269–278; e) J. Shim, A. Coop, A. D. MacKerell, Jr., *J. Phys. Chem. B* **2013**, *117*, 7907–7917; f) B. Trzaskowski, D. Latek, S. Yuan, U. Ghoshdastider, A. Debinski, S. Filipek, *Curr. Med. Chem.* **2012**, *19*, 1090–1109.

[5] a) V. Katritch, G. Fenalti, E. E. Abola, B. L. Roth, V. Cherezov, R. C. Stevens, *Trends Biochem. Sci.* **2014**, *39*, 233–244; b) L. Gelis, S. Wolf, H. Hatt, E. M. Neuhaus, K. Gerwert, *Angew. Chem. Int. Ed.* **2012**, *51*, 1274–1278; *Angew. Chem.* **2012**, *124*, 1300–1304; c) A. Bortolato, B. G. Tehan, M. S. Bodnarchuk, J. W. Essex, J. S. Mason, *J. Chem. Inf. Model.* **2013**, *53*, 1700–1713.

[6] W. Liu, E. Chun, A. A. Thompson, P. Chubukov, F. Xu, V. Katritch, G. W. Han, C. B. Roth, L. H. Heitman, A. P. IJzerman, V. Cherezov, R. C. Stevens, *Science* **2012**, *337*, 232–236.

[7] V. P. Jaakola, M. T. Griffith, M. A. Hanson, V. Cherezov, E. Y. Chien, J. R. Lane, A. P. Ijzerman, R. C. Stevens, *Science* **2008**, *322*, 1211–1217.

[8] a) A. Ohta, M. Sitkovsky, *Nature* **2001**, *414*, 916–920; b) A. S. Doré, N. Robertson, J. C. Errey, I. Ng, K. Hollenstein, B. Tehan, E. Hurrell, K. Bennett, M. Congreve, F. Magnani, C. G. Tate, M. Weir, F. H. Marshall, *Structure* **2011**, *19*, 1283–1293; c) F. Xu, H. Wu, V. Katritch, G. W. Han, K. A. Jacobson, Z. G. Gao, V. Cherezov, R. C. Stevens, *Science* **2011**, *332*, 322–327.

[9] G. Lebon, T. Warne, P. C. Edwards, K. Bennett, C. J. Langmead, A. G. Leslie, C. G. Tate, *Nature* **2011**, *474*, 521–525.

[10] J. A. Ballesteros, H. Weinstein, *Methods Neurosci.* **1995**, *25*, 366–428.

[11] S. D. McAllister, D. P. Hurst, J. Barnett-Norris, D. Lynch, P. H. Reggio, M. E. Abood, *J. Biol. Chem.* **2004**, *279*, 48024–48037.

[12] a) S. Yuan, R. Wu, D. Latek, B. Trzaskowski, S. Filipek, *PLoS Comput. Biol.* **2013**, *9*, e1003261; b) J. Li, A. L. Jonsson, T. Beuming, J. C. Shelley, G. A. Voth, *J. Am. Chem. Soc.* **2013**, *135*, 8749–8759; c) J. Selent, F. Sanz, M. Pastor, G. De Fabritiis, *PLoS Comput. Biol.* **2010**, *6*, e1000884.

[13] a) S. Ye, E. Zaitseva, G. Caltabiano, G. F. Schertler, T. P. Sakmar, X. Deupi, R. Vogel, *Nature* **2010**, *464*, 1386–1389; b) K. Y. Chen, J. Sun, J. S. Salvo, D. Baker, P. Barth, *PLoS Comput. Biol.* **2014**, *10*, e1003636.

[14] H. W. Choe, Y. J. Kim, J. H. Park, T. Morizumi, E. F. Pai, N. Krauss, K. P. Hofmann, P. Scheerer, O. P. Ernst, *Nature* **2011**, *471*, 651–655.

[15] X. Periole, T. Huber, S. J. Marrink, T. P. Sakmar, *J. Am. Chem. Soc.* **2007**, *129*, 10126–10132.

[16] a) H. Sprong, P. van der Sluijs, G. van Meer, *Nat. Rev. Mol. Cell Biol.* **2001**, *2*, 504–513; b) K. Jacobson, O. G. Mouritsen, R. G. Anderson, *Nat. Cell Biol.* **2007**, *9*, 7–14; c) D. Lingwood, K. Simons, *Science* **2010**, *327*, 46–50.

[17] M. G. Wolf, M. Hoefling, C. Aponte-Santamaria, H. Grubmuller, G. Groenhof, *J. Comput. Chem.* **2010**, *31*, 2169–2174.

[18] S. Pronk, S. Pall, R. Schulz, P. Larsson, P. Bjelkmar, R. Apostolov, M. R. Shirts, J. C. Smith, P. M. Kasson, D. van der Spoel, B. Hess, E. Lindahl, *Bioinformatics* **2013**, *29*, 845–854.

[19] a) A. L. Lomize, I. D. Pogozheva, H. I. Mosberg, *J. Chem. Inf. Model.* **2011**, *51*, 918–929; b) A. L. Lomize, I. D. Pogozheva, H. I. Mosberg, *J. Chem. Inf. Model.* **2011**, *51*, 930–946.

[20] K. Lindorff-Larsen, S. Piana, K. Palmo, P. Maragakis, J. L. Klepeis, R. O. Dror, D. E. Shaw, *Proteins Struct. Funct. Bioinf.* **2010**, *78*, 1950–1958.

[21] a) J. P. M. Jämbeck, A. P. Lyubartsev, *J. Phys. Chem. B* **2012**, *116*, 3164–3179; b) J. P. M. Jämbeck, A. P. Lyubartsev, *J. Chem. Theory Comput.* **2012**, *8*, 2938–2948.

[22] V. Zoete, M. A. Cuendet, A. Grosdidier, O. Michielin, *J. Comput. Chem.* **2011**, *32*, 2359–2368.

[23] W. Humphrey, A. Dalke, K. Schulten, *J. Mol. Graph. Model.* **1996**, *14*, 33–38.

[24] O. Beckstein, M. S. Sansom, *Proc. Natl. Acad. Sci. USA* **2003**, *100*, 7063–7068.

[25] A. C. E. Dahl, M. Chavent, M. S. P. Sansom, *Bioinformatics* **2012**, *28*, 2193–2194.

